

Mathematical Model of High-frequency Electromechanical Energy Transducer with High-coercitive Permanent Magnets

Flur Ismagilov, Irek Khayrullin, Vacheslav Vavilov, Aynur Yakupov

Abstract—A mathematical model of a high-frequency electromechanical energy transducer with high-coercitive permanent magnets in cylindrical coordinates is represented in the paper. It allows analyzing magnetic field in the electromechanical energy transducer air gap taking into account temperature fields and mechanical parameters which influence it. The investigations of the mathematical model are conducted and comparisons are found, and inconsistent of the field task solution in the cylindrical and rectangular coordinates is determined.

Keywords—Air gap, High-coercitive permanent magnets (HCPM), High-frequency electromechanical energy transducer (EMET) (EMET).

I. INTRODUCTION

High-frequency electromechanical energy transducers (EMET) with high-coercitive permanent magnets (HCPM) refer to a kind of electric machines characterized by the minimum weight ratio (0,28–0,4 kg/κWt), high efficiency coefficient and reliability [1, 2]. This specifies their application prospects as a main source of electric energy in autonomous object power supply systems, e.g. in flying and space machines, sea crafts and cars [12–18].

Along with that it is impossible to get minimum weight-length parameters at the maximum efficiency coefficient without using new materials which are quite expensive, e.g. carbon fiber for rotor magnets shrouding or soft magnetic alloys with high saturation induction. That is why when designing the EMET with HCPM it is necessary to pay special attention to design calculation accuracy and to take into account a variety of operating factors (which determine the

cost of the EMET). This cannot be done without developing the mathematical model to describe magnetic field in the EMET with HCPM. In several papers including [1–11] mathematical models describing the magnetic field in EMET with HCPM are represented. These models are designed for an EMET with HCPM with a star rotor type, an EMET with the tangentially and radially magnetized HCPM, and an edge-bonded EMET with HCPM. All of them are mathematical descriptions of the magnetic field vector potential in the cylindrical coordinate system. However, HCPM parameters, and resultant magnetic field in the air gap of the EMET with HCPM respectively are under the significant influence of temperature. It is also known that the resultant magnetic field in the EMET air gap depends on the air gap size which is determined mainly by mechanical loads on the rotor bandage case in high-frequency EMETs.

In view of the above the mathematical model describing magnetic field in the specific gap of the high-frequency EMETs with HCPM must factor interrelation of thermal and magnetic fields, and mechanical loads. Thereby, the vital science-based task is to design a mathematical model which will allow analyzing the magnetic field of the air gap of the EMET with HCPM considering interrelations of thermal fields and mechanical parameters with it.

In the first part we calculate the proposed parameters for designing the mathematical model of the EMET with HCPM. The second part is devoted to the estimation of the magnetic field in the air gap of the EMET with HCPM. In the third part the application area of the model is analyzed. In the last part we give the results of several investigations carried out on the EMETs with HCPM.

II. FORMULATION OF THE MATHEMATICAL PROBLEM

While designing the mathematical model the EMET with HCPM is taken, Fig. 1. Moreover, the pattern of 3D magnetic field in the EMET air gap is represented. As there are no currents in the nonmagnetic gap, the magnetic field in the gap is expressed by the Laplace equation in the cylindrical coordinates, in differential coefficient [19]:

$$H_r(r, \varphi, z) = \frac{\partial^2 H_r}{\partial r^2} + \frac{1}{r} \frac{\partial H_r}{\partial r} + \frac{1}{r^2} \frac{\partial^2 H_r}{\partial \varphi^2} + \frac{\partial^2 H_r}{\partial z^2} = 0, \quad (1)$$

Manuscript received January 13, 2016; revised April 25, 2016. Research carried out by the grant Russian Science Foundation (project №16-19-10005).

A. Yakupov is with the Ufa State Aviation Technical University, Ufa, 450008 Russian Federation (corresponding author to provide phone: +79372349921; e-mail: aynurpov@mail.ru).

F. Ismagilov is with the Ufa State Aviation Technical University, Ufa, 450008 Russian Federation (e-mail: ismagilov137@gmail.com).

I. Khayrullin is with the Ufa State Aviation Technical University, Ufa, 450008 Russian Federation (e-mail: irek khayrullin@yandex.com).

V. Vavilov is with the Ufa State Aviation Technical University, Ufa, 450008 Russian Federation (e-mail: s2_88@mail.ru).

$$H_\phi(r, \phi, z) = \frac{\partial^2 H_\phi}{\partial r^2} + \frac{1}{r} \frac{\partial H_\phi}{\partial r} + \frac{1}{r^2} \frac{\partial^2 H_\phi}{\partial \phi^2} + \frac{\partial^2 H_\phi}{\partial z^2} = 0, \quad (2)$$

$$H_z(r, \phi, z) = \frac{\partial^2 H_z}{\partial r^2} + \frac{1}{r} \frac{\partial H_z}{\partial r} + \frac{1}{r^2} \frac{\partial^2 H_z}{\partial \phi^2} + \frac{\partial^2 H_z}{\partial z^2} = 0, \quad (3)$$

where H_r , H_ϕ , H_z are the radial, tangential and axial components of magnetic field intensity, respectively, in the nonmagnetic gap of the EMET with HCPM, r is the geometric parameters of the EMET with HCPM, ϕ is the angle of rotation of the rotor.

Equation system of (1) – (3) can be solved as follows:

$$\text{div} \vec{H} = \frac{1}{r} \frac{\partial H_r}{\partial r} + \frac{1}{r} \frac{\partial H_\phi}{\partial \phi} + \frac{\partial H_z}{\partial z} = 0. \quad (4)$$

As the magnetic field on the HCPM surface depends on the HCPM energetic factors, so the tangential and radial components of the magnetic field on the HCPM surface can be given as follows:

$$H_\phi(r, \phi, z) = k_\phi \frac{J}{4\pi\mu_0} \sin \phi, \quad (5)$$

$$H_r(r, \phi, z) = k_r \frac{J}{4\pi\mu_0} \cos \phi, \quad (6)$$

where k_ϕ is the coefficient of proportionality between the HCPM coercitive force and the HCPM residual induction, and the tangential component of magnetic field intensity on the HCPM surface; J is the HCPM magnetization; k_r is the coefficient of proportionality between the HCPM coercitive force and the HCPM residual induction, and the radial component of magnetic field intensity on the HCPM surface.

Then the interdependence of the thermal and magnetic fields in the air gap will be described by the following equations [20]:

$$B_r(\Theta) = B_r \left(1 - \frac{k_{Br}(\Theta_{\text{HCPM}} - 23)}{100} \right), \quad (7)$$

$$H_c(\Theta) = H_c \left(1 - \frac{k_{Hc}(\Theta_{\text{HCPM}} - 23)}{100} \right), \quad (8)$$

where $B_r(\Theta)$, $H_c(\Theta)$ are effective values of the residual induction and the HCPM coercitive force, respectively; B_r , H_c are values of the residual induction and the HCPM coercitive force given in specifications, respectively; Θ_{HCPM} is the HCPM temperature; k_{Br} is the temperature coefficient of the HCPM residual induction; k_{Hc} is the temperature

coefficient of the HCPM coercitive force.

The air gap value depends on the bandage case load and is calculated as follows:

$$\delta_\sigma = \frac{\Omega^2 \left[\rho_{\text{HCPM}} R_{\text{HCPM}} (D_{\text{HCPM1}}^2 + D_{\text{HCPM2}}^2) \right]}{8\sigma} \quad (9)$$

where Ω is the angular rotation of the EMET with HCPM rotor; ρ_{HCPM} is the HCPM material density; σ is the bandage case ultimate strength to its material yield; R_{HCPM} , D_{HCPM1} , D_{HCPM2} are the geometric parameters of the EMET with HCPM, respectively. F is the mechanical load influencing the rotor bandage case; l is the HCPM effective length.

The geometric parameters are determined according to the Fig. 1:

$$D_{\text{HCPM2}} = D_{\text{HCPM1}} - 2h_M,$$

$$R_{\text{HCPM}} = \frac{D_{\text{max}} - 2\delta_\sigma - h_M}{2}.$$

Boundary conditions and allowances. When solving tasks like this common allowances which do not introduce significant errors into results are used:

I. the core steel magnetic permeability, as well as the shaft steel, is equal to infinity, the air gap magnetic permeability is equal to the vacuum magnetic permeability;

II. the axial component of the magnetic field intensity on the rotor butt end is equal to 0, i.e. the EMET of infinite length is regarded;

III. the nonmagnetic gap value is determined as follows $\delta = \delta_z + \delta_b$ (where δ_b is the rotor bandage case thickness; δ_z is the EMET air gap);

IV. there are no currents in the rotor bandage case and the stator magnetic circuit serration is not calculated;

V. when specifying the rotor bandage case thickness the bandage case weight is not significant in comparison with the HCPM weight;

VI. the EMET shaft temperature is slightly different from the ambient temperature;

VII. the temperature surrounding the EMET is constant.

The allowances mentioned above can be included separately, so the stator serration is calculated by including the Carter factor, buckling flows are calculated by including the design length, and finite permeability becomes the saturation coefficient.

Based on the above allowances the boundary conditions for solving Eq. (1) – (3) can be formulated as follows:

$$H_\varphi \Big|_{r=\frac{D_{HCPM1}+\delta_b}{2}} = 0, \tag{10}$$

$$H_\varphi \Big|_{r=\frac{D_{HCPM1}}{2}} = k_\varphi \frac{J}{4\pi\mu_0} \sin \varphi, \tag{11}$$

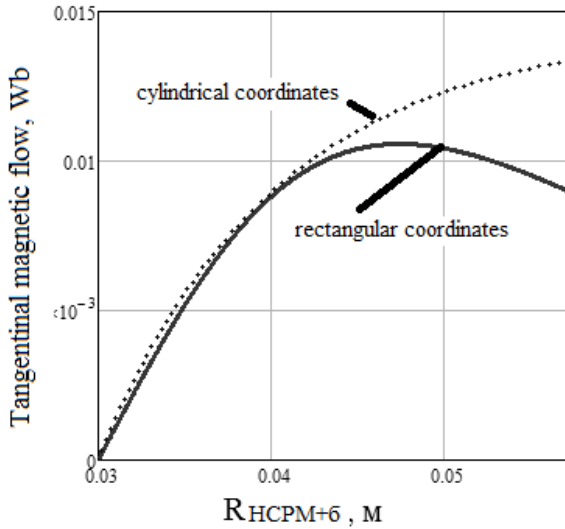


Fig. 1. The tangential magnetic flow designed in the rectangular coordinates system – the air gap changing curve

$$H_r \Big|_{r=\frac{D_{HCPM1}}{2}} = k_r \frac{J}{4\pi\mu_0} \cos \varphi, \tag{12}$$

$$H_z \Big|_{z=0} = 0, \frac{\partial H_z}{\partial z} \Big|_{z=0} = 0, \tag{13}$$

$$H_z \Big|_{z=l}, \frac{\partial H_z}{\partial z} \Big|_{z=l} = 0 \tag{14}$$

The boundary condition (11) is from the allowance I, the boundary conditions (14), (15) are from the allowance II. Moreover, according to the boundary conditions (13), (14) the formulated task becomes the 2D boundary equation for the Laplace equation within the circle using the following radii:

$$\frac{D_{HCPM1}}{2}$$

and

$$\frac{D_{HCPM1} + \delta_b}{2}$$

III. MATHEMATICAL MODEL OF THE EMET WITH HCPM

Considering the boundary conditions the solution for the

magnetic field tangential component in the air gap of the EMET with HCPM can be written as follows:

$$H_\varphi = \frac{A_0}{2} \frac{R_0^{\left(\frac{D_{HCPM1}}{2}\right)}(r)}{R_0^{\left(\frac{D_{HCPM1} + \delta}{2}\right)}} + \sum_{n=1}^{\infty} \frac{R_n^{\left(\frac{D_{HCPM1} + \delta}{2}\right)}(r)}{R_n^{\left(\frac{D_{HCPM1}}{2}\right)}} \{A_n \cos n\varphi + B_n \sin n\varphi\} \tag{15}$$

where

$$R_0^{\left(\frac{D_{HCPM1}}{2}\right)}(r) = \ln \frac{2r}{D_{HCPM1}};$$

$$R_n^{\left(\frac{D_{HCPM1}}{2}\right)}(r) = \frac{-r^{2n} + \left(\frac{D_{HCPM1} + \delta}{2}\right)^{2n}}{r^n};$$

A_0, A_n, B_n are constant components specified by the boundary conditions.

The following values are included:

$$\frac{D_{HCPM1} + 2\delta}{2} = R_{CT}, \tag{16}$$

$$\frac{D_{HCPM1}}{2} = R_{HCPM1}, \tag{17}$$

Considering (16), (17) Eq. (18) can be rewritten in less lengthy form:

$$H_\varphi = \frac{A_0}{2} \frac{R_0^{(R_{HCP1})}(r)}{R_0^{(R_{HCPM})}(R_{CT})} + \sum_{n=1}^{\infty} \frac{R_n^{(R_{CT})}(r)}{R_n^{(R_{CT})}(R_{HCPM})} \{A_n \cos n\varphi + B_n \sin n\varphi\}. \tag{18}$$

From the boundary conditions it is seen that:

If $r = R_{CT}$, then:

$$R_0^{(R_{HCPM})}(r) = \ln \left(1 + \frac{\delta}{D_{HCPM1}} \right);$$

$$R_0^{(R_{HCPM})}(R_{CT}) = \ln \left(1 + \frac{\delta}{D_{HCPM1}} \right);$$

$$R_n^{(R_{HCPM})}(r) = \frac{R_{CT}^{2n} - R_{HCPM1}^{2n}}{R_{CT}^n};$$

$$R_n^{(R_{HCPM})}(R_{CT}) = \frac{R_{CT}^{2n} - R_{HCPM1}^{2n}}{R_{CT}^n}.$$

$$\frac{A_0}{2} + \sum_{n=1}^{\infty} \{A_n \cos n\varphi + B_n \sin n\varphi\} = k_{\varphi} \frac{J}{4\pi\mu_0} \sin \varphi. \quad (19)$$

Thus:

$$A_0 = 0; \quad A_n = 0, \quad n = 1, 2, \dots;$$

$$B_1 = k_{\varphi} \frac{J}{4\pi\mu_0}, \quad B_n = 0, \quad n \neq 1. \quad (20)$$

Using the Eq. (20) we get the following :

$$H_{\varphi}(r, \varphi) = k_{\varphi} \frac{J}{4\pi\mu_0} \frac{(R_{CT}^2 - r^2)R_{HCPM1}}{r(R_{CT}^2 - R_{HCPM1}^2)} \sin \varphi. \quad (21)$$

Coming back to the reverse replacement of (16), (17), Eq. (21) is rewritten as follows:

$$H_{\varphi}(r, \varphi) = k_{\varphi} \frac{J}{4\pi\mu_0} \frac{\left(\left(\frac{D_{HCPM1}}{2} + \delta\right)^2 - r^2\right)\left(\frac{D_{HCPM1}}{2}\right)}{r\left(\left(\frac{D_{HCPM1}}{2} + \delta\right)^2 - \left(\frac{D_{HCPM1}}{2}\right)^2\right)} \sin \varphi \quad (22)$$

Eq. (23) must be checked against the boundary conditions (10), (11):

$$H_{\varphi}\left(\frac{D_{HCPM1}}{2}, \varphi\right) = k_{\varphi} \frac{J}{4\pi\mu_0} \times$$

$$\frac{\left(\left(\frac{D_{HCPM1}}{2} + \delta\right)^2 - \left(\frac{D_{HCPM1}}{2}\right)^2\right)\left(\frac{D_{HCPM1}}{2}\right)}{\left(\frac{D_{HCPM1}}{2}\right)\left(\left(\frac{D_{HCPM1}}{2} + \delta\right)^2 - \left(\frac{D_{HCPM1}}{2}\right)^2\right)} \sin \varphi =$$

$$= k_{\varphi} \frac{J}{4\pi\mu_0} \sin \varphi,$$

$$H_{\varphi}\left(\frac{D_{HCPM1}}{2} + \delta, \varphi\right) = k_{\varphi} \frac{J}{4\pi\mu_0} \times$$

$$\frac{\left(\left(\frac{D_{HCPM1}}{2} + \delta\right)^2 - \left(\frac{D_{HCPM1}}{2} + \delta\right)^2\right)\left(\frac{D_{HCPM1}}{2}\right)}{\left(\frac{D_{HCPM1}}{2} + \delta\right)\left(\left(\frac{D_{HCPM1}}{2} + \delta\right)^2 - \left(\frac{D_{HCPM1}}{2}\right)^2\right)} \sin \varphi = 0.$$

In view of the above the obtained solution corresponds to the specified boundary conditions.

The relationship between the tangential component of the magnetic field intensity in the air gap of the EMET with HCPM and the bandage case mechanical density, and the HCPM temperature is included.

At the same time the relationship between the magnetic field in the HCPM air gap and the temperature can be written based on the following equation:

$$B_r = H_c \mu_0 + J. \quad (23)$$

Considering Eqs (8), (9):

$$J = B_r \left(1 - \frac{k_{Br}(\Theta_{HCPM1} - 23)}{100}\right) - H_c \mu_0 \left(1 - \frac{k_{Hc}(\Theta_{HCPM1} - 23)}{100}\right). \quad (24)$$

$$H_{\phi}(r, \phi) = k_{\phi} \frac{1}{4\pi\mu_0} \left[B_r \left(1 - \frac{k_{Br}(\Theta_{HCPM} - 23)}{100}\right) - H_c \mu_0 \left(1 - \frac{k_{Hc}(\Theta_{HCPM} - 23)}{100}\right) \right] \times$$

$$\frac{\left(\left(\frac{D_{HCPM1}}{2} + \frac{\Omega^2 \left[\rho_{HCPM} R_{HCPM} (D_{HCPM1}^2 + D_{HCPM2}^2)\right]}{8\sigma}\right) - r^2\right)\left(\frac{D_{HCPM1}}{2}\right)}{r\left(\left(\frac{D_{HCPM1}}{2} + \frac{\Omega^2 \left[\rho_{HCPM} R_{HCPM} (D_{HCPM1}^2 + D_{HCPM2}^2)\right]}{8\sigma}\right) - \left(\frac{D_{HCPM1}}{2}\right)^2\right)} \sin \phi, \quad (25)$$

Taking into account Eq. (4) which describes the magnetic field line continuity we can get the following:

$$\frac{1}{r} \frac{\partial H_r r}{\partial r} + \frac{1}{r} \frac{\partial H_\phi}{\partial \phi} = 0, \tag{26}$$

The radial component of the magnetic field intensity in the HCPM nonmagnetic gap is determined as follows:

$$\begin{aligned} \frac{\partial H_r r}{\partial r} = & -k_\phi \frac{1}{4\pi\mu_0} \left[B_r \left(1 - \frac{k_{Br}(\Theta_{HCPM} - 23)}{100} \right) - H_c \mu_0 \left(1 - \frac{k_{Hc}(\Theta_{HCPM} - 23)}{100} \right) \right] \times \\ & \left(\left(\frac{D_{HCPM1}}{2} + \frac{\Omega^2 [\rho_{HCPM} R_{HCPM} (D_{HCPM1}^2 + D_{HCPM2}^2)]}{8\sigma} \right)^2 - r^2 \right) \left(\frac{D_{HCPM1}}{2} \right) \\ & \times \frac{\cos \phi}{r \left(\left(\frac{D_{HCPM1}}{2} + \frac{\Omega^2 [\rho_{HCPM} R_{HCPM} (D_{HCPM1}^2 + D_{HCPM2}^2)]}{8\sigma} \right)^2 - \left(\frac{D_{HCPM1}}{2} \right)^2 \right)} \end{aligned} \tag{27}$$

If two parts of the equation are divided into r , then:

$$\begin{aligned} \partial H_r = & -k_\phi \frac{1}{4\pi\mu_0 r} \left[B_r \left(1 - \frac{k_{Br}(\Theta_{HCPM} - 23)}{100} \right) - H_c \mu_0 \left(1 - \frac{k_{Hc}(\Theta_{HCPM} - 23)}{100} \right) \right] \times \\ & \left(\left(\frac{D_{HCPM1}}{2} + \frac{\Omega^2 [\rho_{HCPM} R_{HCPM} (D_{HCPM1}^2 + D_{HCPM2}^2)]}{8\sigma} \right)^2 - r^2 \right) \left(\frac{D_{HCPM1}}{2} \right) \\ & \times \frac{\cos \phi \partial r}{r \left(\left(\frac{D_{HCPM1}}{2} + \frac{\Omega^2 [\rho_{HCPM} R_{HCPM} (D_{HCPM1}^2 + D_{HCPM2}^2)]}{8\sigma} \right)^2 - \left(\frac{D_{HCPM1}}{2} \right)^2 \right)} \end{aligned} \tag{28}$$

To find the magnetic field radial component in the air gap of the EMET with HCPM the integral from the right and left parts is taken. Moreover, the factors which do not depend on H_r and r , put outside the integral sign:

$$\begin{aligned} \int \partial H_r = & -k_\phi \frac{1}{4\pi\mu_0} \left[B_r \left(1 - \frac{k_{Br}(\Theta_{HCPM} - 23)}{100} \right) - H_c \mu_0 \left(1 - \frac{k_{Hc}(\Theta_{HCPM} - 23)}{100} \right) \right] \times \\ & \left(\frac{D_{HCPM1}}{2} \right) \\ & \times \frac{\cos \phi \times}{\left(\left(\frac{D_{HCPM1}}{2} + \frac{\Omega^2 [\rho_{HCPM} R_{HCPM} (D_{HCPM1}^2 + D_{HCPM2}^2)]}{8\sigma} \right)^2 - \left(\frac{D_{HCPM1}}{2} \right)^2 \right)} \\ & \times \int \frac{\left(\left(\frac{D_{HCPM1}}{2} + \frac{\Omega^2 [\rho_{HCPM} R_{HCPM} (D_{HCPM1}^2 + D_{HCPM2}^2)]}{8\sigma} \right)^2 - r^2 \right) \partial r}{r^2} \end{aligned} \tag{29}$$

By integrating both parts of Eq. (29):

$$\begin{aligned}
 H_r + C_1 = & -k_\phi \frac{1}{4\pi\mu_0} \left[B_r \left(1 - \frac{k_{Br}(\Theta_{HCPM} - 23)}{100} \right) - H_c \mu_0 \left(1 - \frac{k_{Hc}(\Theta_{HCPM} - 23)}{100} \right) \right] \times \\
 & \left(\frac{D_{HCPM1}}{2} \right) \\
 & \times \frac{\cos \phi \times \left(\left(\frac{D_{HCPM1}}{2} + \frac{\Omega^2 [\rho_{HCPM} R_{HCPM} (D_{HCPM1}^2 + D_{HCPM2}^2)]}{8\sigma} \right)^2 - \left(\frac{D_{HCPM1}}{2} \right)^2 \right)}{\left(\left(\frac{D_{HCPM1}}{2} + \frac{\Omega^2 [\rho_{HCPM} R_{HCPM} (D_{HCPM1}^2 + D_{HCPM2}^2)]}{8\sigma} \right)^2 \right)} \\
 & \times \left(r - \frac{\left(\left(\frac{D_{HCPM1}}{2} + \frac{\Omega^2 [\rho_{HCPM} R_{HCPM} (D_{HCPM1}^2 + D_{HCPM2}^2)]}{8\sigma} \right)^2 \right)}{r} \right) + C_2
 \end{aligned} \tag{30}$$

From the boundary condition (12):

$$C_1 - C_2 = -\frac{J}{4\pi\mu_0} \cos \phi (k_\phi + k_r) \tag{31}$$

Then including (32), Eq. (31) can be rewritten as follows:

$$\begin{aligned}
 H_r - \frac{J}{4\pi\mu_0} (k_\phi + k_r) \cos \phi = & -k_\phi \frac{1}{4\pi\mu_0} \left[B_r \left(1 - \frac{k_{Br}(\Theta_{HCPM} - 23)}{100} \right) - H_c \mu_0 \left(1 - \frac{k_{Hc}(\Theta_{HCPM} - 23)}{100} \right) \right] \times \\
 & \left(\frac{D_{HCPM1}}{2} \right) \\
 & \times \frac{\cos \phi \times \left(\left(\frac{D_{HCPM1}}{2} + \frac{\Omega^2 [\rho_{HCPM} R_{HCPM} (D_{HCPM1}^2 + D_{HCPM2}^2)]}{8\sigma} \right)^2 - \left(\frac{D_{HCPM1}}{2} \right)^2 \right)}{\left(\left(\frac{D_{HCPM1}}{2} + \frac{\Omega^2 [\rho_{HCPM} R_{HCPM} (D_{HCPM1}^2 + D_{HCPM2}^2)]}{8\sigma} \right)^2 \right)} \\
 & \times \left(r - \frac{\left(\left(\frac{D_{HCPM1}}{2} + \frac{\Omega^2 [\rho_{HCPM} R_{HCPM} (D_{HCPM1}^2 + D_{HCPM2}^2)]}{8\sigma} \right)^2 \right)}{r} \right)
 \end{aligned} \tag{32}$$

Taking the similar additive component:

$$H_r(r, \varphi) = \frac{\cos \varphi}{4\pi\mu_0} \left[B_r \left(1 - \frac{k_{Br}(\Theta_{HCPM} - 23)}{100} \right) - H_c \mu_0 \left(1 - \frac{k_{Hc}(\Theta_{HCPM} - 23)}{100} \right) \right] \left\{ -k_\varphi \times \right. \\ \left. \times \frac{\left(\frac{D_{BIM1}}{2} \right)}{\left(\left(\frac{D_{HCPM1}}{2} + \frac{\Omega^2 [\rho_{HCPM} R_{HCPM} (D_{HCPM1}^2 + D_{HCPM2}^2)]}{8\sigma} \right)^2 - \left(\frac{D_{HCPM1}}{2} \right)^2 \right)} \times \right. \\ \left. \times \left(r - \frac{\left(\left(\frac{D_{HCPM1}}{2} + \frac{\Omega^2 [\rho_{HCPM} R_{HCPM} (D_{HCPM1}^2 + D_{HCPM2}^2)]}{8\sigma} \right)^2 \right)}{r} \right) + k_\varphi + k_r \right. \quad (33)$$

So a set of Eqs (24)-(32) is the mathematical model which describes the magnetic field in the air gap of the EMET with HCPM taking into account interrelations of the EMET active parts temperature and the magnetic fields, as well as the mechanical load on the rotor bandage.

IV. APPLICATION AREA OF THE DESIGNED MATHEMATICAL MODEL

In the paper [21] the task on specifying the 3D magnetic field in the nonmagnetic gap of the EMET with HCPM is solved by using the Laplace equation in the differential coefficient in the rectangular coordinates:

$$H_z = H_{z0m} (\text{ch}q_3 z - \text{th}q_3 \delta \text{sh}q_3 z) \cos q_1 x \cos q_2 y, \quad (35)$$

$$H_x = -H_{z0m} \frac{q_3}{q_1 + q_2} \text{ch}q_3 z (\text{th}q_3 \delta - \text{th}q_3 z) \times \\ \times \sin q_1 x \cos q_2 y \quad (36)$$

$$H_y = -H_{z0m} \frac{q_3}{q_1 + q_2} \text{ch}q_3 z (\text{th}q_3 \delta - \text{th}q_3 z) \times \\ \times \cos q_1 x \cos q_2 y \quad (37)$$

where $q_1 = \frac{\pi}{\tau}$, $q_2 = \frac{\pi}{l}$, $q_3 = \sqrt{q_1^2 + q_2^2}$, τ is the EMET polar pitch.

The solutions mentioned above are less lengthy than the obtained equations with the air gap flexion. Therefore, it is reasonable to analyze discrepancies and find application areas for Eqs (35)–(37).

When analyzing the discrepancies between the solutions in the rectangular and cylindrical coordinates the relationships of the tangential and radial magnetic flow (z and x used in Eqs (35)–(37)) and the air gap value for the EMET with the rotor diameter of 60 mm and the effective length of 180 mm are calculated. Comparative analysis of the calculation results for the tangential magnetic flow is shown in Fig. 2.

Having analyzed Fig. 2 it is seen that in the close gaps sphere up to 4 mm discrepancies in solutions for the cylindrical coordinates system and rectangular coordinates

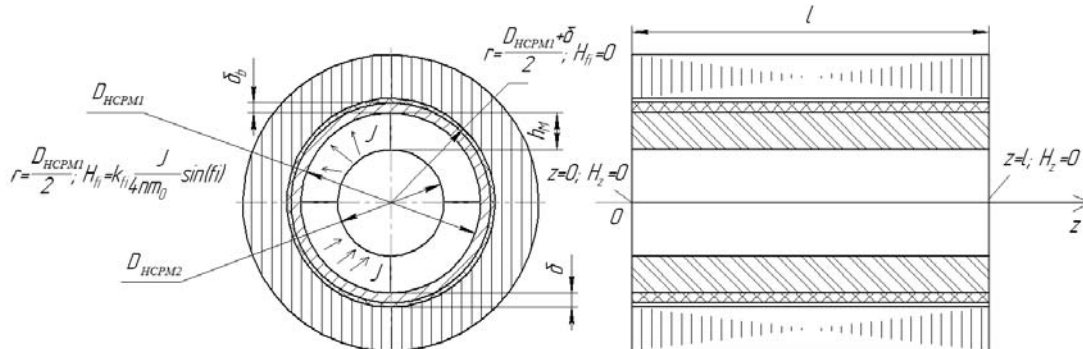


Fig. 2. Design model of the EMET with HCPM

system do not exceed 5%. In the sphere of the air gap value more than 4 mm discrepancies in solutions for the cylindrical coordinates system and rectangular coordinates system reach 30%. For the radial magnetic flow the results have the similar nature. Thus it is obvious that for the gap not more than 4 mm Eqs (35)–(37) can be used, at the gap more than 4 mm the air gap flexion must be considered.

V. ELECTROMECHANICAL TRANSDUCER INVESTIGATIONS BY USE OF THE DESIGNED MATHEMATICAL MODEL

On the basis of the designed mathematical model the multiple investigations of the EMET with HCPM have been conducted; the actions of temperature and mechanical strength on its parameters have been estimated, i.e. applicability of the designed mathematical model is shown in the paper.

In Figs 3, 4, 5 the interdependence between the magnetic flow radial component in the air gap of the high-speed EMET with HCPM and the temperature, air-gap distance and other parameters put on the HCPM.

From the curve (Fig. 3) it is seen that if the air-gap increases as twice the magnetic flow R-component amplitude decreases to 1,85; and if the air-gap is up by 28,5 per cent the magnetic flow R-component amplitude in the air-gap of the EMET with HCPM is down by 66 per cent.

While plotting the curve in Fig. 5 constant temperature coefficients for HCPM of different types are used. Herewith the curve 5 shows that HCPM temperature influences the magnetic flow R-component in the air-gap significantly. So, for the HCPM of NdFeB type if the temperature increases from 70 to 140 degrees the magnetic flow R-component is down to 25-35 per cent. In spite of the fact that the initial characteristics of NdFeB 38UH type (at the temperature of 230C) are higher than those of Sm2Co17 type (if the residual induction is 10 per cent more, coercitive force is up to 7-8 per cent, while at the temperature of 230C the HCPM of NdFeB 38UH type creates radial magnetic flow which is by 9 per cent more than the HCPM of Sm2Co17 type). So at the temperature of 700C the parameters of the HCPM of Sm2Co17 and of NdFeB 38UH types become equal and create the similar magnetic flows, at the temperature of 140-1500C the HCPMs of Sm2Co17 type create the magnetic flow in the air-gap of the EMET with HCPM by 20 per cent more than the HCPM of NdFeB 38UH type. Therefore it is reasonable to use the HCPM of NdFeB type in the EMET with HCPM in cases when their temperature does not exceed 500C, however in other cases it is more reasonable to use the HCPM of Sm2Co17 type for purposes of providing energetic characteristics.

Therefore, the designed mathematical model allows conducting multiple investigations of the EMET with HCPM parameters.

VI CONCLUSION

In the paper the mathematical model describing the magnetic field in air gap of the electromechanical energy transducers with high-coercitive permanent magnets is

designed. Interrelations between the EMET active parts temperature and the magnetic fields and the mechanical strength are taken into account. The research has shown that:

- if the air gap increases as twice, the tangential magnetic flow in the air gap of the EMET with HCPM goes up to 40–45 %. Moreover, with the air gap increase the tangential magnetic flow will rise according to its height. Herewith the radial magnetic flow decreases to 7–8 %, i.e. if the air gap increases in the EMET with HCPM then penetration of the magnetic field radial component in the EMET decreases and weakening action of the tangential component increases.
- in the close gaps sphere up to 4 mm discrepancies in solutions for the cylindrical coordinates system and rectangular coordinates system do not exceed 5%. In the

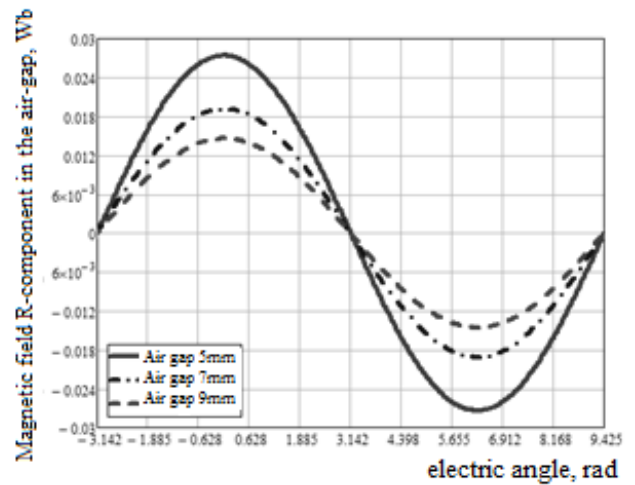


Fig. 3. The magnetic field R-component in the air gap of the high-speed EMET with HCPM – the air-gap distance curve

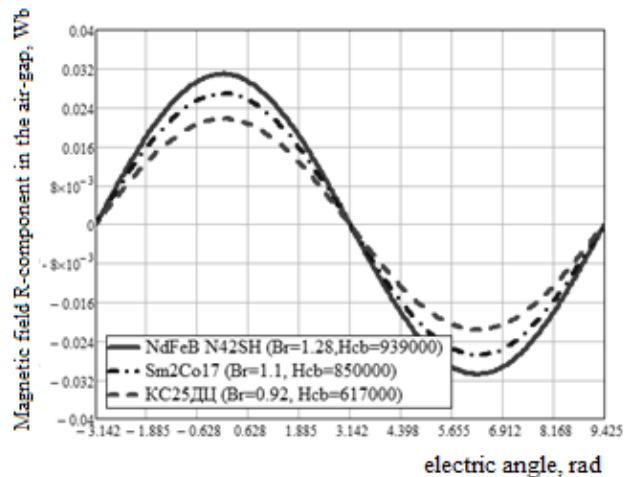


Fig. 4. The magnetic flow R-component in the air-gap of the high-speed EMET with HCPM – the HCPM type curve

sphere of air gap value more than 4 mm discrepancies in solutions for the cylindrical coordinates system and rectangular coordinates system reach 30%. Consequently, it is obvious that for the gap not more than 4 mm the magnetic field in the air gap can be calculated without including the flexion, at the gap more than 4 mm the air gap flexion must be considered.

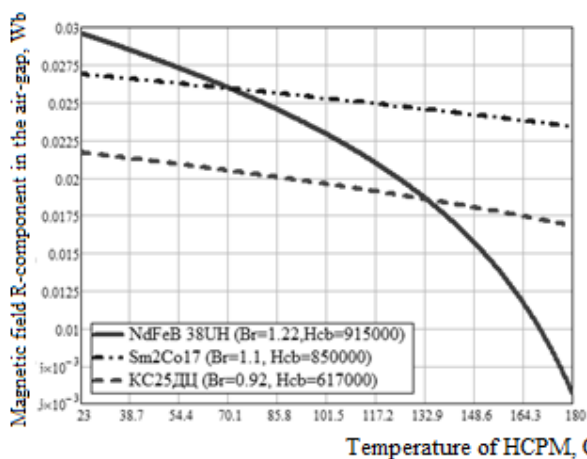


Fig.5. The magnetic flow R-component in the air-gap of the high-speed EMET with HCPM - the HCPM temperature for different types of HCPM at the electric angle equal to 0 curve

ACKNOWLEDGMENT

Research carried out by the grant Russian Science Foundation (project №16-19-10005).

REFERENCES

- [1] R. Ravaund, G. Lemarquand, V. Lemarquand, "Force and Stiffness of Passive Magnetic Bearings Using Permanent Magnets." Part 1: Axial Magnetization, *IEEE Transactions on Magnetics*. 2009. V.45 . I. 7. pp.2996–3002, doi: 10.1109/TMAG.2009.2016088
- [2] R Ravaund, G. Lemarquand, V. Lemarquand, "Analytical Calculation of the Magnetic Field Created by Permanent-Magnet Rings,"*IEEE Transactions on Magnetics*. 2008. v.44. n. 8. p.1982–1989.
- [3] Li W., X. Zhang, S. Cheng, "Thermal Optimization for a HSPMG Used for Distributed Generation Systems,"*IEEE Transactions on Industrial Electronics*. 2013. Vol. 60 № 2. pp. 474–482.
- [4] Rakotoarison, H., J. Yonnet, and B. Delinchant, "Using coulombian approach for modelling scalar potential and magnetic field of a permanent magnet with radial polarization," *IEEE Transactions on Magnetics*, Vol. 43, No. 4, pp.1261–1264, Apr. 2007.
- [5] Zhilichev, Y., "Calculation of magnetic field of tubular permanent magnet assemblies in cylindrical bipolar coordinates,"*IEEE Transactions on Magnetics*, Vol. 43, No. 7, pp.3189–3195, Jul. 2007.
- [6] Lindell, I. V., "Electromagnetic field in self-dual media in different-form representation,"*Progress In Electromagnetics Research, PIER* 58, pp.319–333, 2006.
- [7] Azzerboni, B. and E. Cardelli, "Magnetic field evaluation for disk conductors,"*IEEE Transactions on Magnetics*, Vol. 29, No. 6, pp.2419–2421, 1993.
- [8] Xu, X. B. and L. Zeng, "Ferromagnetic cylinders in earth's magnetic field: A two-dimensional model of magnetization of submarine,"*Progress In Electromagnetics Research, PIER* 19, pp.319–335, 1998.
- [9] Babic, S. I. and C. Akyel, "New mutual inductance calculation of the magnetically coupled coils: Thin disk coil-thin wall solenoid," *Journal of Electromagnetic Waves and Applications*, Vol. 20, No. 10, pp.1661–1669, 2006.
- [10] Lemarquand, G. and V. Lemarquand, "Annular magnet position sensor,"*IEEE Transactions on Magnetics*, Vol. 26, No. 5, 2041–2043, Sep. 1990.
- [11] Lemarquand, G. and V. Lemarquand, "Variable magnetic torque sensor," *J. Appl. Phys.*, Vol. 70, No. 10, pp.6630–6632, 1991.
- [12] Pulyer, Y. and M. Hrovat, "Generation of remote homogeneous magnetic fields," *IEEE Transactions on Magnetics*, Vol. 38, No. 3, pp.1553–1563, May 2002.
- [13] Berkouk, M., V. Lemarquand, and G. Lemarquand, "Analytical calculation of ironless loudspeaker motors," *IEEE Transactions on Magnetics*, Vol. 37, No. 2, pp.1011–1014, Mar. 2001.

- [14] Abdi, B., Bahrami, H., Ghiasi, M.I., Ghasemi, R., PM machine optimization in variable speed EMB application, (2012) *International Review of Electrical Engineering (IREE)*, 7 (3), pp. 4412-4418.
- [15] Li, Z., Magnetic field analysis of a novel deflection-type PM multi-DOF actuator, (2013) *International Review of Electrical Engineering (IREE)*, 8 (1), pp. 89-95.
- [16] Huijuan Liu, Yue Hao, ShuangxiaNiu, Weinong Fu Computation of Electromagnetic Losses in Double-Rotor Vernier PM Motors with Three Topologies Using TS-FEM, *International Review of Electrical Engineering (IREE)* Vol 10, No 1 (2015)
- [17] Zhongda Tian, Shujiang Li, Yanhong Wang, and Quan Zhang, "Multi Permanent Magnet Synchronous Motor Synchronization Control based on Variable Universe Fuzzy PI Method," *Engineering Letters*, vol. 23, no.3, pp180-188, 2015
- [18] P. Pao-la-or, A. Isaramongkolrak, T. Kulworawanichpong, "Finite Element Analysis of Magnetic Field Distribution for 500-kV Power Transmission Systems," *Engineering Letters*, vol. 18, no.1, pp1-9, 2010
- [19] A. Ghoggal, M. Sahraoui, and S.E Zouzou A Comprehensive, "Method for the Modeling of Axial Air-gap Eccentricities in Induction Motors," *Engineering Letters*, vol. 17, no.2, pp45-53, 2009
- [20] Minos Beniakar, Themistoklis Kefalas, Kladas A. Investigan of the Impact of the Operational Temperature of a Surface Permanent Magnet Motor // *Materials Science Forum*. 2011. Vol. 670. P. 259–264
- [21] Gerasin A., Ismagilov F., Vavilov V. Electromechanical systems with highly coercive permanent magnets // *Moscow, Mechanical Engineering*, 2014.-262 with. ISBN 978-5-94275-755-7

Flur R. Ismagilov – Prof., Head of the Department of Electromechanics, Ufa State Aviation Technical University (Ufa), tel+7 (347) 273-77-87

Vacheslav E. Vavilov – P.h.D., Lecturer of the Department of Electromechanics, Ufa State Aviation Technical University (Ufa), tel. 89273465305, e-mail: s2_88@mail.ru.

Irek H. Khayrullin – Prof., the Department of Electromechanics, Ufa State Aviation Technical University (Ufa).

Aynur M. Yakupov – Post-graduate student, Engineer at the Department of Electromechanics, Ufa State Aviation Technical University (Ufa); e-mail: aynurpov@mail.ru; address: 158/1, Mingajeva Str, Apt. 507, Ufa, Russia, 450000 (zip code).